Published in final edited form as:
Dev Biol. 2012 April 15; 364(2): 138–148. doi:10.1016/j.ydbio.2012.01.025.

Nuclear localization of Prickle2 is required to establish cell polarity during early mouse embryogenesis

Hirotaka Tao[a,b], **Ken-ichi Inoue**[a], **Hiroshi Kiyonari**[a], **Alexander G. Bassuk**[c,d], **Jeffrey D. Axelrod**[e], **Hiroshi Sasaki**[f,g], **Shinichi Aizawa**[a,h], and **Naoto Ueno**[b,i,*]

[a]Laboratory for Animal Resources and Genetic Engineering, RIKEN Center for Developmental Biology (CDB), 2-2-3 Minatojima-minamimachi, Chuo-ku, Kobe 650-047, Japan

[b]Division of Morphogenesis, National institute for Basic Biology, 38 Nishigonaka, Myoudaiji, Okazaki 444-8585, Japan

[c]Department of Pediatrics, University of Iowa, Iowa City, IA 52242, USA

[d]Department of Neurology, University of Iowa, Iowa City, IA 52242, USA

[e]Department of Pathology, Stanford University school of Medicine, Stanford, CA 94305, USA

[f]Laboratory for Embryonic induction, RIKEN Center for Developmental Biology (CDB), 2-2-3 Minatojima-minamimachi, Chuo-ku, Kobe 650-047, Japan

[g]Department of Cell Fate Control, Institute of Molecular Embryology and Genetics, Kumamoto University, 2-2-1 Honjo, Kumamoto 860-0811, Japan

[h]Laboratory for Vertebrate Body Plan, RIKEN Center for Developmental Biology (CDB), 2-2-3 Minatojima-minamimachi, Chuo-ku, Kobe 650-047, Japan

[i]Department of Basic Biology, School of Life Science, Graduate University of Advanced Studies (SOKENDAI), 38 Nishigonaka, Myodaiji, Okazaki 444-8585, Japan

Abstract

The establishment of trophectoderm (TE) manifests as the formation of epithelium, and is dependent on many structural and regulatory components that are commonly found and function in many epithelial tissues. However, the mechanism of TE formation is currently not well understood. *Prickle1 (Pk1)*, a core component of the planar cell polarity (PCP) pathway, is essential for epiblast polarization before gastrulation, yet the roles of *Pk* family members in early mouse embryogenesis are obscure. Here we found that $Pk2^{-/-}$ embryos died at E3.0–3.5 without forming the blastocyst cavity and not maintained epithelial integrity of TE. These phenotypes were due to loss of the apical-basal (AB) polarity that underlies the asymmetric redistribution of microtubule networks and proper accumulation of AB polarity components on each membrane during compaction. In addition, we found GTP-bound active form of nuclear RhoA was decreased in $Pk2^{-/-}$ embryos during compaction. We further show that the first cell fate decision was disrupted in $Pk2^{-/-}$ embryos. Interestingly, Pk2 localized to the nucleus from the 2-cell to around the 16-cell stage despite its cytoplasmic function previously reported. Inhibiting farnesylation blocked Pk2's nuclear localization and disrupted AB cell polarity, suggesting that Pk2

*Correspondence: nueno@nibb.ac.jp.

farnesylation is essential for its nuclear localization and function. The cell polarity phenotype was efficiently rescued by nuclear but not cytoplasmic *Pk2*, demonstrating the nuclear localization of Pk2 is critical for its function.

Introduction

In preimplantation mouse development, the first cell lineages to be established are the trophectoderm (TE) and inner cell mass (ICM) (Marikawa and Alarcón, 2009; Rossant and Tam, 2009; Sasaki, 2010; Zernicka-Goetz, 2009). In mouse, these lineages begin to diverge at the 8-cell stage, when blastomeres polarize during compaction. In this process, blastomeres acquire apical-basal (AB) polarity, typified by the apical localization of microvilli and acquisition of cytoplasmic polarity, including the asymmetric distribution of E-cadherin and reorganization of the microtubule (MT) network (Fleming and Johnson, 1988; Jonson et al., 1986; Maro et al., 1990). Next, the blastocoel, a fluid-filled cavity, is formed in the central region of the embryonic cell mass. Blastocoel formation requires two major interrelated features of TE differentiation: intracellular junction biogenesis and a directed transport system, mediated by Na^+/K^+ ATPase (Eckert and Fleming, 2008). These findings suggest that the functional polarity of embryonic cells is essential for proper blastocyst cavity formation. The cell polarity complex (aPKC/PAR) regulates the orientation of cell cleavage planes and cell polarity (Alarcón, 2010; Dard et al., 2009; Plusa et al, 2005). Thus, the aPKC/PAR complex also influences the localization of blastomeres to an outer or inner position in the blastocyst as well as blastocoel formation (Alarcón, 2010; Plusa et al, 2005). However, the connection between these two processes is unclear.

Planar cell polarity (PCP) is manifested as the coordinated, polarized orientation of cells within epithelial sheets, or as the directional cell migration and intercalation during convergent extension (Axelrod, 2009; Goodrich and Strutt, 2011; Simons and Mlodzik, 2008; Zallen, 2007). The signaling pathway that controls PCP consists of *Celsr/Flamingo*, *Frizzled* (*Fzd*), *Dishevelled* (*Dvl/Dsh*), *Van Gogh/strabisumus* (*Vang/stbm*), *Diego*, and *Prickle* (*Pk*). The PCP pathway is proposed to modulate the cytoskeleton and influence cell morphology rather than cell fates in many cases (Wansleeben and Meijlink, 2011). Nevertheless, some PCP components are essential for asymmetric cell division and cell fate determination during mouse neurogenesis (Goodrich, 2008; Lake and Sokol, 2009). Furthermore, some PCP components appear to participate in multiple pathways and to create crosstalk with other pathways such as that for AB determination, suggesting that some PCP genes have acquired new functions that exploit their fundamental properties in PCP signaling (Goodrich, 2008; Goodrich and Strutt; 2011; Nishita et al., 2010; Wansleeben amd Meijlink, 2011).

Two *prickle* (*pk*) genes, *Pk1* and *Pk2*, have been identified in the mouse (Katoh and Katoh, 2003), and the deletion of *Pk1* revealed its early developmental role of *Pk1* in establishing the AB polarity of the epiblast (Tao et al., 2009). In addition, the mouse PCP core component *Vangl2* interacts genetically with *Scribble* (*Scrib*) (whose *Drosophila* orthologue regulates AB polarity) in determining the planar polarity of inner cell cilia (Montcouquiol et al., 2003, 2006). Together, these results highlight a functional link between the PCP and AB polarity systems (Nishita et al., 2010). On the other hand, the apical determinants *aPKC* and *PARD6b* regulate cell lineage during mouse preimplantation development (Alarcón, 2010; Dard et al., 2009; Plusa et al., 2005), although their roles in controlling TE differentiation and blastocyst formation are still unclear. The functional relationship between PCP components and aPKC/PAR complex proteins, the key players in AB polarity formation, are also unclear. However, evidence suggests that aPKC phosphorylates and inhibits the activity of Fzd to regulate PCP in the *Drosophila* eye (Djiane et al., 2005) and Dvl is involved in

establishment of AB polarity by binding to and regulating the activity of Lgl, a target of aPKC in *Xenopus* (Dollar et al., 2005).

In this article, we show that Pk2 is expressed throughout mouse preimplantation development and regulates AB cell polarity during compaction, thus also regulating the first cell fate decision. The *Pk2*$^{-/-}$ embryos showed arrested development at the late morula stage, failed to form the blastocyst cavity, and at the late 8-cell stage, showed defects in microtubule network redistribution and Na^+/K^+ ATPase α1 subunit accumulation on the basolateral membrane. Furthermore, nuclear-targeted but not cytoplasmically localized Pk2 rescued the polarity defect phenotypes, indicating that nuclear retention of Pk2 is essential for its function. We provide the first evidence that Pk2 plays a crucial role in mouse preimplantation development and highlight the functional link between AB polarity establishment and PCP pathway.

Materials and methods

Mice

Pk2 mutant mice were generated as described (Tao et al., 2011). Two *Pk2* mutant mouse strains (line1, #64 and line 2, #134) were established from independent homologous recombinant ES cells, and no difference in preimplantation phenotype (defective formation of blastocyst cavity) was apparent between them (Table S1A). Unless stated otherwise, all of experiments were carried out with line 2 mice. For pre-implantation embryos, genotyping was performed on individually isolated embryos directly or after observation in culture of following antibody staining. *Vangl2*$^{Lp/+}$ mice (strain LPT/LeJ) were obtained from The Jackson Laboratory and maintained by backcrossing to C57BL/6J. Inbred C57BL/6J were purchased from LARGE (RIKEN CDB) or CLEA CO., LTD., Japan. Inbred CBA strains were purchased from Oriental Yeast CO., LTD. and Charles River CO., LTD. Mice were housed in environmentally controlled rooms at the NIBB and/or RIKEN CDB, under the institutional guidelines for animal and recombinant DNA experiments, respectively.

Embryo collection and in vitro culture

The preimplantation embryos were collected from timed natural matings or *in vitro* fertilization pre-Embryo transfer (IVF-ET). The preimplantation embryos were collected by flushing dissected oviducts or uteri with M2 medium (M7167, Sigma) with HEPES (M7167, Sigma). Embryos were cultured in 80 μl drops of KSOM (ARK Resource Co., Ltd.) under mineral oil (M8410, Sigma) at 37°C in a 5% CO_2 incubator. The inhibitor treatment was performed in 3.5 cm dish (Nunc). Embryos with or without the zona pellucida were cultured in 80–160ul drops containing several dose of inhibitors and covered with mineral oil. Details of antibodies and inhibitors are shown in Table S2.

Whole-mount immunofluorescence

Embryos were fixed in 4% paraformaldehyde (PFA) in phosphate-buffered saline (PBS) for 15–30 min at room temperature, and then embryos were treated with acidified Tyrode's solution (T1788, SIGMA) to remove the zona-pellucida. Embryos were subsequently permeabilized with 0.2% Triton X-100 in PBS for 20 min at room temperature, washed in PBSS for 5 min, blocked with 2% goat serum in PBS (blocking solution), and incubated overnight with primary antibodies diluted in blocking solution at 4°C. The Primary antibodies lists were provided in Table S2. After washing in PBSS for 15 min, 3 times, embryos were incubated with the following secondary antibodies diluted in PBSS for 1 hr at room temperature: Alexa Fluor 488 goat anti-rabbit, goat anti-mouse, donkey anti-goat (A11034, A11029, A11055; 1:1000–4000, Molecular Probes) and/or Alexa Fluor 555 goat anti-rabbit, goat anti-mouse, goat anti-rat (A21428, A21422, A21434; 1:1000–4000,

Molecular Probes). Embryos were washed in PBSS and postfix in 4% PFA/PBS. Then, embryos were placed in a drop of 40% glycerol/PBS or PermaFluor aqueous mounting medium (TA-030-FM, Thermo Scientific) on a glass-bottom dish (D110400, Matsunami).

Microscopy and image analysis

Laser scanning microscopy was performed using LSM 510 Meta, LSM 710 ZEN and LSM 780 ZEN (Zeiss), with optical sections obtained approximately every 3–5μm. The relative fluorescence of intensity in each picture was measured by ImageJ, and accounts between value 0 and 255. These indices were based on a pixel-based quantitative analysis of confocal images. The obtained relative fluorescence intensity profiles were transferred into Microsoft EXCEL for further quantification. Same blastomeres with more intense nuclear than cytoplasmic staining were considered positive. The images shown in some of the figures were modified using contrast enhancement or and brightness (Adobe Photoshop CS4). Statistically significant differences (* $p < 0.05$, ** $p < 0.01$) are indicated by asterisks.

Immunoblotting

Embryos were treated with acidified Tyrode's solution (T1788, SIGMA) to remove the zona-pellucida. Three sets of 100–200 embryo pools were used for preparation of protein extracts separately. Embryos were collected in a sample buffer (x4 ME, Wako) (62.5mM Tris-HCl at pH6.8, 0.5x PBS, 2% SDS, 10% Glycerol, 5% 2-mercaptothanol), and then sonicated to cleave genomic DNA. The nuclear and cytoplasmic extracts were separated by using Nuclear/cytosol fractionation kit (K266-25, BIOVISON), following the manufacturer's instructions. These proteins were denatured by heating at 95°C for 5 min, separated by electrophoresis on SDS-5% polyacrylamide gels, and transfered onto Immobilon (IPVH20200, Millipore). Blots were blocked with 5% skimmed milk, incubated overnight with primary antibodies at 4°C. After several washes, blots were incubated with a 1:10,00 dilution of HRP-conjugated anti-rabbit IgG antibody, and detected by using ECL Advance Western Blotting Detection Kit (RPN2106, GE Healthcare) and LAS3000 lumino-image analyzer (Fuji).

Construction of plasmids

The full-length coding sequences of mouse *Pk1* (ID A630056F08) and *Pk2* (ID M5C1081L03) were amplified from RIKEN FANTOM cDNA library. The Myc-tagged *Prickle2* and various myc tagged *Prickle2* mutant expression vectors were constructed with 6xMyc pCAGGS or 6xMyc pcDNA3.1 poly (Yamagata et al., 2005) vectors, respectively. For mutagenesis, the specific primer used with the KOD -Plus- mutagenesis kit (SMK-101, TOYOBO) are shown in Table S3A. Theses oligo cDNAs were performed by Operon Biotechnologies, Japan.

Reverse Transcription-PCR (RT-PCR)

The total *RNAs* were isolated from individual embryos using TRIzol plus RNA purification kit (#12183-555, Invitrogen) following the manufacturer's instruction. All of total *RNA* was used for cDNA synthesis using Superscript III reverse transcriptase (#18080-044, Invitrogen) following the manufacturer's instruction. The resultant cDNA was diluted appropriately for semi-quantitative PCR. Primers used are shown in Table S3B.

DNA and RNA Injection and In Vitro mRNA Transcription

Poly(A)-tailed *RNA* was synthesized from several cDNAs cloned into the pcDNA3.1-poly(A)83 plasmid (Yamagata et al., 2005) and *in vitro* transcription was performed using the mMESSAGE mMACHINE T7 and Sp6 kit (AM1344 and AM1340, Ambion). Synthesized *RNAs* were purified by NucAway Spin Columns (AM10070, Ambion) and

dissolved in water and −20°C before microinjection. The purified *RNAs* were injected into both blastomeres of 2-cell-stage embryos according to standard protocols (Nagy et al., 2003). The DNAs were injected in pronuclei of 1-cell stage embryos according to standard protocols (Nagy et al., 2003).

Rho-GTP affinity assay

Analysis of active Rho protein was conducted as previously described (Xie et al., 2008). Briefly, embryos were fixed with freshly prepared 2% PFA in PBS for 20 minutes at room temperature. After washing, embryos were permeabilized in PBS containing 3% BSA, 0.1 M glycine and 0.05% Triton X-100, followed with blocking in the same buffer containing 2% donkey serum, then incubated with 50 μg/ml GST tagged Rhotekin-RBD (RT01A, Cytoskelton) for 2 hours at 4°C. Anti-GST primary (1:200, B-14, Santa Cruz) and secondary antibodies were used to visualize the GST-GTP-bound active Rho proteins.

Results

Expression and subcellular localization of Pk2 protein during preimplantation development

To investigate whether *Pk2* is involved in preimplantation development, we first examined the expression and subcellular localization of the Pk2 protein in MII oocytes and preimplantation embryos by immunostaining with an anti-Pk2-specific antibody (Figs. 1A-F). Pk2 protein was undetectable in MII oocytes (n = 23/23) (Fig. 1A), and was first detected in the nucleus of 2-cell-stage embryos (n = 17/18) (Figs. 1B and B'). The nuclear signal became stronger until the 8–16-cell stage (n > 15 embryos, respectively) (Figs. 1B-D'; Fig. S1A), suggesting that Pk2 is not maternally expressed but produced only in the embryo. To distinguish whether maternal or zygotic transcripts produce Pk2, we treated embryos from the late 1-cell to the 4-cell stage with 0.1 mg/ml α-amanitine (α-AM), an inhibitor of RNA polymerase II, and therefore of zygotic gene activation (Hamatani et al., 2004) (Fig. S2). In most of the α-AM-treated embryos, nuclear Pk2 signals were absent (2-cell stage; n = 21/21, 4-cell stage, n = 19/22) (Figs. S2D, D', F and F'), suggesting that the Pk2 protein is not maternally expressed. From the 16-cell stage onwards, the nuclear Pk2 signal decreased as the cytoplasmic Pk2 signal increased (n > 20 blastomeres, n = 5 embryos, respectively) (Figs. 1E and E'; Figs. S1A, C and D), an observation that was confirmed by western blotting of nuclear and cytoplasmic extracts from compacted 8-cell stage and blastocyst stage embryos (Fig. S1B). Pk1, the other *prickle* family gene in the mouse, was also expressed in the nucleus of all blastomeres from the 2-cell to the blastocyst stage, as shown by immunostaining with an anti-Pk1-specific antibody (n > 20 embryos, respectively) (Fig. S3A). Notably, Pk2 was mostly localized to the nuclei of embryonic cells up to the 16-cell stage, and primarily before blastocyst formation, but Pk1 remained in the nuclei at the blastocyst stage.

Background-dependent embryonic lethality in $Pk2^{-/-}$ mouse embryos

To study the *in vivo* function of *Pk2*, we generated knock-out mice lacking PET/LIM, one of the functional domains of *Pk2* (Tao et al., 2011). In the $Pk2^{-/-}$ embryos, no Pk2 protein was observed at the 8-cell stage (n = 8/8) (Fig. S3B), while the localization and expression level of Pk1 was not affected (n = 5/5), compared with $Pk2^{+/+}$ and $Pk2^{+/-}$ (control) embryos (n = 23/23) (Fig. S3C). Two independent Pk2 homozygous mutant alleles displayed similar defective formation of blastocyst cavity on the C57BL/6 x CBA mixed background (Table S1A). After crossing pairs of $Pk2^{+/-}$ mice, we did not find any $Pk2^{-/-}$ mice on the CBA background (Tables S1B and C), suggesting the homozygous mutation was lethal in early embryonic development. However, when the $Pk2^{+/-}$ mice were backcrossed with C57BL/6 over 6 generations, the $Pk2^{-/-}$ progenies were viable and fertile (Table S1D), although they

had a slightly reduced body size and an epilepsy-like neuronal disorder as we recently reported (Tao et al., 2011). We assume that the presence of modifier genes for *Pk* function underlies these background-dependent phenotypes.

Pk2$^{-/-}$ embryos failed to form a blastocyst cavity

To reveal abnormalities in the *Pk2*$^{-/-}$ embryos, we first examined their preimplantation development. The *Pk2*$^{-/-}$ embryos underwent compaction at the late 8-cell stage and were morphologically indistinguishable from controls up to the 25–30-cells stage (Figs. 1G and J). Subsequently, the *Pk2*$^{-/-}$ embryos failed to form a definitive blastocyst cavity, and instead maintained a morula-like morphology (Figs. 1H and K). Up to the late blastocyst stage, *Pk2*$^{-/-}$ embryos started to exhibit small cell fragments on the surface (Figs. 1I and L). The number of nuclei in *Pk2*$^{-/-}$ embryos was significantly decreased compared with that in controls at the early blastocyst stage (Fig. 1M), indicating that the cell proliferation of *Pk2*$^{-/-}$ embryos was arrested or cell death occurred. To test for cell death, we immunocytochemically examined cleavage-stage embryos for cleaved caspase-3, which faithfully represents the execution of apoptosis. The results showed that the *Pk2*$^{-/-}$ embryos progressed beyond the 16-cell stage, but then the number of cleaved caspase-3 positive cells gradually increased throughout the embryo (n = 8/8) (Figs. S4A-E).

Pk2 affects TE lineage specification

Next, we asked if the differentiation of TE/ICM is affected in *Pk2*$^{-/-}$ embryos. *Cdx2* is the key factor in TE-fate specification (Plusa et al., 2005; Strumpf et al., 2005). *Tead4*, the TEA domain transcription factor, was recently identified as an essential factor for TE development acting upstream of *Cdx2* (Yagi et al., 2007; Nishioka et al., 2008, 2009). *Tead4*$^{-/-}$ embryos do not express Cdx2, fail to form a blastocyst cavity, and all the cells follow the ICM fate (Yagi et al., 2007; Nishioka et al., 2008). To address whether *Pk2* is involved in this cell-differentiation process, we first examined the expression of YAP1, the Tead4 co-activator protein, and Cdx2 in *Pk2*$^{-/-}$ embryos (Figs. 2A, B, D and E; Figs. S5A-D). In the *Pk2*$^{-/-}$ embryos, the expression of YAP1 and Cdx2 was observed at the 14–16-cell stage (n = 6/6, respectively) (Figs. S5A-D). After the next cell division, however, the nuclear Yap1 and Cdx2 signals disappeared from most cells in the *Pk2*$^{-/-}$ embryos (n = 9/9, respectively) (Figs. 2A-F).

Although the outer cells of the *Pk2*$^{-/-}$ embryos were morphologically distinct (flattened) from the inner cells at 13–15-cell stage, it was still possible that the outer cells have adopted an ICM fate, as was reported for *Cdx2*$^{-/-}$ blastomeres that inappropriately express Nanog and Oct3/4 (Strumpf et al., 2005). Therefore, we examined the expression of Nanog and Oct3/4 in *Pk2*$^{-/-}$ embryos (Figs. S5E-H). At 13–15-cell stage, expression levels of Nanog and Oct3/4 in the *Pk2*$^{-/-}$ embryos were indistinguishable from those in controls (n = 9/10, n = 4/4) (Figs. S5E-H). *Cdx2*$^{-/-}$ mutants develop into early blastocysts, but the blastocoel eventually collapses (Strumpf et al., 2005). In this mutant, the expression of TE-specific genes significantly decreases, and all the cells are positive for Nanog in early blastocyst (Strumpf et al., 2005). *Tead4*$^{-/-}$ mutants, and *Pard6b siRNA*-injected embryos (Alarcón, 2010; Nishioka et al., 2008) show similar phenotypes to *Cdx2*$^{-/-}$. Likewise, in *Pk2*$^{-/-}$ embryos at 26–29-cell stage, the ratio of Nanog-positive blastomeres/total blastomeres was significantly increased compared with controls (n = 11/14) (Figs. 2A', B', D', E' and G).

Moreover, RT-PCR analysis at the late morula stage revealed the absence of transcripts of *Yap1* and *Cdx2*, and upregulated *Nanog* expression in the *Pk2*$^{-/-}$ embryos (Fig. 2H), indicating that *Pk2* is essential for the specification and development of TE possibly through the proper establishment of cell polarity and maintenance of gene expression of *Yap1* and *Cdx2*.

Pk2 mediates the proper positioning of Pericentriolar Material 1 (PCM1) and microtubule (MT) redistribution within the cell cortex during compaction

We next examined whether *Pk2* regulates the asymmetric reorganization of the MT network and/or the accumulation of cell-cell contact via E-cadherin during compaction as markers for epithelial polarity formation. In control and $Pk2^{-/-}$ non compacted-8-cell blastomeres, the MT meshwork was found mainly around the nucleus and at the cell cortex (n = 8) (Figs. S6A-B'), whereas pericentriolar material 1 (PCM1), a major component of the centriole, was diffused in the cytoplasm (n = 4) (Figs. S6C and D). During compaction, the MTs accumulated in the apical part of cell and decreased in the basal domain (Figs. 3B, D and F). In contrast, the $Pk2^{-/-}$ blastomeres exhibited an irregular α-tubulin-staining pattern, with a dispersed MT network, and no distinct organization (n = 8/9) (Figs. 3C, E and G), although E-cadherin localized fairly normally to the AJs (n = 12/12) (Fig. 3H; Figs. S6E and F). In most of the $Pk2^{-/-}$ blastomeres, α-tubulin staining showed an irregular local deposition at the apical cell surface, and accumulated at intercellular contact points, as compared with controls (Figs. 3B-H). These findings revealed that assembly of MT meshwork at the cell cortex was perturbed in the $Pk2^{-/-}$ blastomeres, although phalloidin staining that marks F-actin were normal in $Pk2^{-/-}$ embryos at the 8–12-cell stage (Figs. 3I-J2).

During compaction, the majority of PCM1 puncta accumulate at the apical domain of the controls (Figs. S6G and G'), where PCM1acts as a microtubule-organizing center (MTOC) in blastomeres (Houliston et al., 1987). By contrast, aberrant aggregates of PCM1 were often observed in the apical part of $Pk2^{-/-}$ blastomeres (27/32 blastomeres, n = 4) (Figs. S6H and H'). Interestingly, tyrosinated tubulin, a microvillus structural component, was dispersed, in part, on the apical membrane of $Pk2^{-/-}$ blastomeres (19/24 blastomeres, n = 3) (Figs. S6I and J). Together these findings indicated that the loss of epithelial polarity was accompanied by a delocalization of the microtubular network.

RhoA activity is decreased in $Pk2^{-/-}$ embryos

We next examined the possible defects in signaling pathways of $Pk2^{-/-}$ embryos during compaction. Recent studies showed that Wnt-c-jun N-terminal kinase (JNK) signaling and Ras-MAPK signaling are required for cavity formation (Lu et al., 2008; Xie et al., 2008). In $Pk2^{-/-}$ embryos, there were no significant effects on the apical membrane localization of Erk2, which is the downstream effector of Ras-MAPK signaling, β-catenin, or the nuclear localization of phosphorylated c-Jun, a JNK substrate protein (n = 3/3 in each case) (Figs. S7A-F).

Vangl2/stbm is a homolog of the *Drosophila* PCP gene *Vangl/stbm*, and its function is closely related to *pk*'s in *zebrafish* gastrulation cell movements (Carreira-Barbosa et al., 2003). At the compacted 8-cell stage, the localization of Vangl2 was not affected in $Pk2^{-/-}$ embryos (n = 4/5) (Figs. S7G and H). To investigate whether *Pk2* and *Vangl2/stbm* act cooperatively in the preimplantation embryo, we crossed $Pk2^{+/-}$ female mice to *Looptail* ($Vangl2^{Lp/+}$) males, *Vangl2* hypomorphic mutants. The double heterozygous mutant embryos formed a normal blastocyst cavity indistinguishable from wild-type embryos (Fig. S7I). Although the penetrance of the phenotype appeared to vary with the genetic background, the result was in contrast to the interaction of these genes in the establishment of cell polarity in the inner ear (Deans et al., 2007).

Rho proteins are required for the maintenance of microtubule orientation (Clayton et al., 1999). We thus performed an *in situ* Rho-GTP affinity assay (Xie et al., 2008) to examine the RhoA activity in the $Pk2^{-/-}$ embryo. The nuclear signals of total and GTP-bound (active) RhoA GTPase were dramatically decreased at the 8–16-cell stage in $Pk2^{-/-}$

embryos (n = 9/10, for both) (Figs. 3K-N), suggesting that Pk2 regulates microtubules orientation via the activation of Rho family GTPase in preimplantation embryos.

Disrupted expression and localization of aPKC/PAR and Scribble complex in Pk2$^{-/-}$ embryos

The abnormal microtubule orientation during compaction suggested that *Pk2* acts as an AB polarity determinant in the early mouse embryo. To test this hypothesis, we investigated the localization of several polarity components in the blastomeres during compaction, focusing on the aPKC/PAR complex, which plays a role in establishing cell polarity and cell division orientation in many other systems (Suzuki and Ohno, 2006). We first examined the expression and localization of PARD6b, a Par6 homolog, and an atypical PKC, PKCζ. Both aPKC and Par complex adopt a polarized localization from the 8-cell stage onwards; manipulating their function re-directs cell positioning and consequently influences cell fate (Alarcón 2010; Dard et al., 2009; Plusa et al., 2005). We found that, at compacted 8-cell stage of control embryos, significant portions of PARD6b and phosphorylated PKCζ (p-PKCζ) were observed at the apical pole of newly polarized cells (n > 30 embryos, respectively) (Figs. 4A, C and E; Fig. S8A). Notably, on the apical cell surface in *Pk2*$^{-/-}$ embryos, this distribution of PARD6b, p-PKCζ and PKCζ was, respectively, lost and partially reduced (n = 5 for both) (Figs. 4B, D and E; Figs. S8A and B). The fluorescence intensity of nuclear PARD6b was also significantly reduced in the *Pk2*$^{-/-}$ blastomeres (22/24 blastomeres, n = 3 embryos) (Fig. 4F). As the loss of Pk2 affect both apical membrane and nuclear localization of PARD6b, Pk2 may functionally interact with PARD6b.

In a variety of polarized cells, the aPKC/PAR complex and PAR-1/EMK1 exhibit complementary localizations along the polarity axis of each cell (Suzuki and Ohno, 2006). At the compacted 8–12-cell stage, EMK1 was mostly found in the nucleus and weakly distributed at the membrane (Vinot et al., 2005) (Figs. 4G and I; Fig. S8C). In the *Pk2*$^{-/-}$ embryos, much of the EMK1 was reduced from cell-cell contacts (n = 3/5) (Figs. 4H, J and K; Fig. S8C).

Since the Scribble complex (Scribble and Lethal giant larvae) has an essential but context-dependent role in regulating the directed cell migration and establishment of AB polarity in epithelial cells of other systems (Nelson, 2009; Suzuki and Ohno, 2006), we investigated the expression and localization of the Scribble (Scrib) and Lethal giant larvae homolog 1 (Lgl1) proteins. At compacted 8–12-cell stage, Scrib was dispersed from the basolateral membrane in the *Pk2*$^{-/-}$ embryos (n = 3/4), while it remained at regions of cell-cell contact in controls (Figs. 4L and M; Fig. S8D). In contrast, Lgl1 retained its normal basolateral distribution in most *Pk2*$^{-/-}$ blastomeres (n = 3/4) (Figs. 4P and Q; Fig. S8E). Interestingly, Scrib and Lgl1 were co-localized with Na^+/K^+ ATPase α1 subunit whose function is essential for blastocyst cavity formation, along the basolateral membranes at the compacted 8-cell stage (n > 15 embryos, respectively) (Figs. 4L, N, P and R; Figs. S8D and E). Similar to Scrib, Na^+/K^+ ATPase α1 was also disrupted at the basolateral membrane in *Pk2*$^{-/-}$ embryos (n = 8/8) (Figs. 4O and S; Figs. S8D and E). Together, these results suggested that *Pk2* is required to establish the AB polarity of outer cells during compaction, which is prerequisite for blastocyst cavity formation.

Farnesyltransferase inhibitor treatment disrupts cell polarity and blocks the nuclear localization of Pk2 in embryos

We next examined which functional domains of *Pk2* are required for preimplantation development. The prenylation motif at the C-terminus of *Pk* is known to be necessary for its function (Mapp et al., 2011; Shimojo and Hersh, 2003, 2006). Prenylation mediated by

farnesyltransferase (FT) or geranylgeranyltransferase (GGT) attaches isoprenyl anchors to C-terminal motifs in substrate proteins (Maurer-Stroh et al., 2007). In addition, preimplantation embryos treated with mevastatin, an HMG CoA reductase inhibitor that blocks prenylation, show arrested development around the late morula stage (Surani et al., 1983).

To address how the nuclear localization of Pk2 affects cell polarity, we treated late 4-cell-stage mouse embryos with an FT inhibitor, B581, or GGT inhibitor, GGTI-298, by adding it to the culture medium (Fig. S9A). The FT inhibitor-treated embryos showed disruptions in ZO-1 and PARD3 localization (n = 4/6, n = 12/14, respectively) (Fig. S9B). After 18 hrs, many of the FT inhibitor-treated embryos became arrested and maintained a morula-like morphology, while the DMSO-treated embryos formed a blastocyst cavity (n = 88/96) (Fig. S9C). These data suggested that FT activity is required to maintain epithelial integrity during preimplantation development. Late 4-cell-stage embryos treated with a GGT inhibitor were morphologically indistinguishable from DMSO-treated control embryos (n = 32/42) (Fig. S9C).

Interestingly, the nuclear signal of Pk2 was decreased in the 8-cell embryos treated with 10 μM FT inhibitor B581 for 8 hrs (n = 12/12) (Fig. S9D). To confirm this finding biochemically, we performed western blots of nuclear and cytoplasmic fractions obtained from DMSO- and FT inhibitor-treated embryos at the late 8-cell stage (Fig. S9E). These data suggested that farnesylation is essential for its nuclear localization and thus for preimplantation development. Next, we examined the subcellular localization of myc-tagged *Pk2 ΔCIIS*, in which the farnesylation motif (CIIS) was deleted, and myc-tagged full-length *Pk2* by injecting their respective *mRNAs* into each blastomere of wild-type 2-cell-stage embryos (Figs. S10A and C). The injection of 5 ng/μl full-length *Pk2 mRNA* did not affect cell polarity or cause developmental arrest, compared with EGFP-injected embryos (Figs. S10C and D). However, an excess amount (50 ng/μl) of full-length *Pk2 mRNA* caused developmental retardation or arrest (Fig. S10C), whereas the injection of 10 ng/μl or 50 ng/μl full-length *Pk1 mRNA* did not affect cell polarity (n = 30/30, n = 25/25) (Fig. S11A). Myc-tagged-*Pk2* was localized to the nucleus (Fig. S10D), and myc tagged-*Pk2 ΔCIIS* was localized to the cytoplasm (n = 12/12) (Fig. S10D). Notably, *Prickle2 ΔCIIS RNA* caused developmental arrest even at a low dose (5 ng/μl) (Fig. S10C), suggesting that the excess cytoplasmic Pk2 interrupts normal development. These data demonstrated that the CIIS motif of *Pk2* is required for its nuclear localization, and together with the result of FT inhibitor-treatment, suggested that loss of the nuclear Pk2 signal prevents cell polarization during compaction.

The nuclear retention of Pk2 is required for the establishment of cell polarity

To further test the hypothesis that farnesylation of Pk2 is critical for cell polarization and for the nuclear localization of Pk2 during preimplantation development, we replaced the 15 C-terminal residues of *Pk2* with the sequence for farnesylation identified in *Lamin B1* (*Pk2ΔFT-Lamin B1*) or *Kras2b* (*Pk2ΔFT-Kras2b*), each targeting Lamin B1 and KRAS2B to nucleus and cytoplasm/plasma membrane, respectively (Fig. S10A) (Maurer-Stroh et al., 2007). At the 8-cell stage, Lamin B1 was present at the nuclear envelope and KRAS2b was distributed in a punctate pattern throughout the cytoplasm (Fig. S10B). The localizations of endogenous Pk2 and Lamin B1 or KRAS2b were not altered in embryos injected with *RNA* encoding *Pk2ΔFT-LaminB1* or *Pk2ΔFT-Kras2b*, respectively (n > 10 in each case) (Fig. S10B). To correlate cellular distribution of Pk2 with its function, *RNA* encoding myc-tagged forms of the above constructs were injected into each blastomere of wild-type 2-cell stage embryos and analyzed by immunofluorescence confocal microscopy with an anti-myc antibody (Fig. S10E). *Pk2ΔFT-Lamin B1*-injected embryos showed the nuclear localization of myc and disruption of the apical PKCζ localization at 14–18-cell stage (n = 19/21) (Fig.

S10E). In *Pk2ΔFT-Kras2b*-injected embryos, myc staining showing a cytoplasmic localization, and the apical PKCζ localization was disrupted at 14–18-cell stage (n = 17/18) (Fig. S10E). The injection of 5 ng/μl *Pk2ΔFT-Lamin B1* or *Pk2ΔFT-Kras2b caused* developmental arrest, compared with 5 ng/μl full-length *Pk2*-injected embryos (Fig. S10F). These data suggested that the overexpression of Pk2 in either the nucleus or cytoplasm disrupts cell polarity during compaction and proper development.

We next tested cellular localization-function relationship of Pk2 and asked whether *Pk2ΔFT-Lamin B1* or *Pk2ΔFT-Kras2b* could rescue the cellular phenotypes of $Pk2^{-/-}$ embryos (Fig. 5). The myc-tagged full-length *Pk2 RNA*-injected embryos and myc-tagged *Pk2ΔFT-Lamin B1 RNA*-injected embryos showed the nuclear localization of myc at the compacted 8-cell stage in $Pk2^{-/-}$ embryos (n = 4/4, n = 3/3) (Figs. 5A and B). In myc-tagged *Pk2ΔFT-Kras2b RNA*-injected embryos, myc staining showed a cytoplasmic localization (n = 3/3) (Fig. 5C). In embryos injected with 5 ng/μl full-length *Pk2 RNA* and *Pk2ΔFT-Lamin B1 RNA*, PKCζ, PARD6b and Scrib were located in membrane at the compacted 8–12-cell stage in the $Pk2^{-/-}$ embryos (*Pk2*; n = 4/4, 6/6 and 4/5, *Pk2ΔFT-Lamin B1*; n = 3/3, 4/5 and 5/6) (Figs. 5D, E, G, H, J-K'), suggesting that the cell polarity defect had been rescued as we expected. In contrast, cytoplasmically retained *Pk2* (*Pk2ΔFT-Kras2b*) failed to rescue (PKCζ, PARD6b and Scrib; n = 8/8, 6/7 and 6/8) (Figs. 5F, I, L and L'). In addition, the injection of 10 ng/μl or 50 ng/μl full-length *Pk1* cDNA into the pronuclei never restored apical localization of PKCζ and formed a blastocyst cavity in $Pk2^{-/-}$ embryos (Fig. S11B and C), suggesting again that Pk2, but not Pk1, can affect the polarization of blastomeres. Importantly, the MT network of the apical part of $Pk2^{-/-}$ blastomeres rescued with the full-length *Pk2* or nuclear-targeted *Pk2* was indistinguishable from that of wild-type blastomeres (*Pk2*; n = 5/5, *Pk2ΔFT-Lamin B1*; n = 5/6) (Figs. 5M and N), although cytoplasmically retained *Pk2* failed to restore the disruption of α-tubulin staining (*Pk2ΔFT-Kras2b*; n = 8/8) (Fig. 5O). Together, these results suggest that nuclear translocation of Pk2 is prerequisite to its function in establishing the cell polarity of early blastomeres and that the loss of epithelial polarity was accompanied by a delocalization of the MT network.

Discussion

Here we demonstrated new roles of *Pk2* in controlling the redistribution of the MT network during compaction and of functional proteins that are normally asymmetrically localized, both of which depend on the establishment of AB polarity. Misregulation of these events by *Pk2* gene knockout leads to aberrant positional information and thus to inappropriate cell fate decisions. These results provide the first evidence that *Pk2* plays a crucial role in mouse preimplantation development.

Intriguingly, these phenotypes are only seen predominantly CBA background on which almost all of $Pk2^{-/-}$ embryos die before implantation due to the loss of zygotic Pk2. However, when the chimeras were backcrossed with C57BL/6 mice over a few generations, $Pk2^{-/-}$ mutant mice started to survive. Although less commonly observed as a general situation, it is possible that modifier gene(s) are involved in controlling embryo survival and thus in increasing viability. These results also rule out the possibility that the phenotypic diversity of Pk2 is due to a difference between the C57BL/6 and CBA strains in either the *Pk2* gene itself or a closely linked gene. We would reason that interactions of Pk with various interacting proteins could be differently affected in C57BL/6 and CBA strains. The presence as well as the number of modifier genes involved in this variation of preimplantation phenotype will be unveiled by a precise genetic mapping.

Models for cell fate determination in the early mouse embryo include the “Inside-Outside” model, in which topological differences dictate cell fates, and the polarity model, in which a differential inheritance of information along the AB axis dictates both cell position and fate (Marikawa and Alarcón, 2009; Sasaki, 2010; Yamanaka et al., 2006). Consistent with the polarity model, the presence of polarity promotes adoption of the TE fate (Alarcón, 2010; Jedrusik et al., 2008; Nishioka et al., 2008, 2009; Plusa et al., 2005). In the present study, *Pk2*$^{-/-}$ embryos showed aberrant AB polarity during compaction, and then, at the late morula stage, nuclear signals of YAP1 and/or Cdx2 were almost completely lost. Interestingly, nuclear localization of YAP1 seems to be disappeared altogether rather than relocating to the cytoplasm in outer cells of *Pk2*$^{-/-}$ embryos at 26–28-cell stage. These results led us to speculate how *Pk2* regulates *YAP1* transcription. Previous reports (Alarcón, 2010; Nishioka, 2008, 2009) together with our results suggest that *Pk2* regulates a Tead4-Cdx2-dependent pathway for TE development, supporting the polarity model. However, a significant difference between *Pk2*$^{-/-}$ and *Tead4*$^{-/-}$ embryos is that the former impairs PKCζ localization (our study) and latter does not (Nishioka et al., 2008). The difference may be the result of additional roles of Pk2 in polarization of TE. Therefore, our result also suggests the possibility that *Pk2* regulates this process either upstream or independently from *Tead4*.

Obviously, it is important to clarify how the cell polarization and transcriptional factors-based mechanisms are connected. Thus, we can assume two possibilities about this concern. First, Tead4 activity is regulated by cell-cell contact through a Hippo signaling pathway components (Nishioka et al., 2009), and the Crumbs polarity complex interacts with YAP (Varelas et al., 2010). These reports presented a model in which cell-cell contact controls transcriptional factor-mediated TE determination. In our study, the EMK1, Na^+/K^+ ATPase α1, and Scrib localizations on the basolateral membrane were disrupted in *Pk2*$^{-/-}$ embryos before the first cell fate decision, suggesting a possible functional relationship between these polarity components and *Pk2*. Second, it has been reported a model in which Cdx2 is involved in cell polarization process (Jedrusik et al., 2008, 2010), and there is a positive feedback loop between Cdx2 and cell polarization (Jedrusik et al., 2008, 2010; Ralston and Rossant, 2008). It is noteworthy that *Cdx2* mRNA and cell polarity molecules (e.g. aPKC) become localized apically at 8- and 16-cell stage (Plusa et al., 2005; Ralston and Rossant, 2008; Vinot et al., 2005). Importantly, Cdx2 depletion by injection of *Cdx2* RNAi at 2-cell stage caused strongly down-regulation of PKCζ expression at the 8- and 16-cell stage (Jedrusik et al., 2010), reminiscent of *Pk2*$^{-/-}$ phenotype. Moreover, in *Pk2*$^{-/-}$ embryos, apical localization of PKCζ does not rescue by injection of cytoplasmic Pk2. These results reveal that Pk2 may participate as the molecular machinery, which is relationship of Cdx2 and aPKC localization. Interestingly, in *Pk2*$^{-/-}$ embryos, nuclear Cdx2 is heterogeneity at 14–16-cell stage, and a similar distribution was also observed in the wild-type embryos. Taken together, these observations suggested that although loss of Pk2 impaired apical-basal polarity during compaction, which indirectly led to the failure of up-regulation in Cdx2 expression during first cell fate decision process.

Next, in this study, we mainly focused on cellular distribution at 8–16-cell stage, which is compaction is taking place. Compaction is mediated by at least two pathways, cell-cell contact mediated by E-cadherin-dependent adherence, and MT-mediated interactions between the nuclei and the cell surface, which result in the formation of the polarized (flattened) epithelium (Fleming and Johnson, 1988; Johnson et al., 1986; Maro et al., 1990). Here we showed that cell-cell adhesion, indicated by localization of E-cadherin and β-catenin, was not hardly affected in *Pk2*$^{-/-}$ embryos. Moreover, *Pk2*$^{-/-}$ embryos did not show obvious differences in Lgl1 localization. These results are supported by a previous report that Lgl is dispensable for the basolateral and tight junctional localization of β-catenin and β1-integrin (Dollar et al., 2005). Thus, the loss of *Pk2* influenced neither the Lgl1

localization nor the cell adhesion via E-cadherin and/or β-catenin during cell polarization. On the other hand, our observation that compaction occurs with disorganized/misoriented MTs and PCM suggested that rather than being the driving force for polarization of the 8-cell blastomere, MTs might coordinate the compaction process and reinforce the asymmetry already established at the cell periphery (Our study, (Houliston and Maro, 1989)). Nevertheless, our data show that the loss of Pk2 may influence the stabilization of centrosomes and MTs, with effects on epithelial cell organization during early mouse development. In contrast, a recent report showed that the MT cytoskeleton is needed for the establishment, but not the maintenance, of the anterior Pk localization of the mesodermal cells during *zebrafish* gastrulation (Sepich et al., 2011). This report suggested that MT dynamics is tightly linked to Pk function. In any case, we speculate that Pk2 may be an essential component of vesicular membrane transport and membrane polarization through MT-based motility.

Rho GTPases play a role in establishing polarity in mouse blastomeres during compaction (Clayton et al., 1999). In the $Pk2^{-/-}$ embryos, the total and active RhoA were reduced around the time of compaction, and the phenotypes were similar to those of RhoA-injected embryos, i.e., disrupted MTs and relatively normal E-cadherin (Clayton et al., 1999). Such similarities of gain- and loss-of-function phenotypes are often observed for both RhoA and PCP components (Takeuchi et al., 2003; Veeman et al., 2003), and they suggest that the tuning of these activities to the proper levels is crucial. The actual role of PCP signaling is somewhat unclear, but these results reveal that a functional correlation between Pk2 and RhoA signaling for the establishment of cell polarity.

In this study, we showed that *Pk2's* C-terminal prenylation by farnesyltransferase is required for nuclear localization of Pk2. Consistent with this, HMG-CoA reductase, which acts upstream of FT and GGT and whose gene is activated from morula to the blastocyst stage (Hamatani et al., 2004) was reported to be essential for mouse preimplantation development (Surani et al., 1983). These observations strongly suggest that in early mouse development, the Pk2 protein is farnesylated and its activity is tightly regulated. Beside early embryogenesis, farnesylation and nuclear localization of *Pk1b* which is more similar to mouse *Pk1* in *zebrafish* have recently reported to be essential for facial branchiomotor neuron (FBMN) migration (Mapp et al., 2011), suggesting that the post-translational modification of *Pk* is an evolutionarily conserved and broadly occurring event.

We also showed that a nucleus- but not a cytoplasm-targeted *Pk2* mutant could rescue cell polarization, demonstrating that its protein product was functional in nucleus. This may suggest that cell polarity establishment requires the physical exclusion of Pk2 from the cytoplasm, at least in the early cleavage stages. Although these showed that nuclear localization of Pk2 is necessary and sufficient for the establishment of AB cell polarity, how the polarity information is transmitted from the nucleus to the membrane remains to be investigated. One possibility is that Pk may function in transcriptional regulation. Pk1, which is also known as RILP (REST (RE-1 silencing transcription factor) interacting LIM domain protein), is associated with the transcriptional repressor REST in other systems (Bassuk et al., 2008; Mapp, et al., 2011; Shimojo and Hersh, 2003, 2006). REST also appears to promote pluripotency by repressing multiple components of the Wnt pathway in mouse embryonic stem cells (Johnson et al., 2008). To understand *Pk2*'s contribution to transcriptional control, global gene expression analyses should be performed.

In conclusion, our results reveal a new role for the polarity molecule *Pk2* in the establishment of AB cell polarity and cell fate decision, particularly with respect to proper formation of the blastocyst. We have also been able to demonstrate that nuclear localization of Pk2 is the key process, which is somewhat unexpected from cytoplasmic function of Pks

which had been broadly recognized. As the Hippo signaling pathway has recently emerged as a novel pathway regulating cell polarity formation and the first cell fate decision during preimplantation development, it is intriguing to investigate crosstalk between this pathway and the PCP signaling pathway to understand how the epithelial architecture is achieved.

Supplementary Material

Refer to Web version on PubMed Central for supplementary material.

Acknowledgments

We thank Dr. V.B. Alarcon (University of Hawaii) and Dr. Y. Marikawa (University of Hawaii) for critical discussion. We are grateful to the Laboratory for Animal Resources and Genetic Engineering staff for collecting mouse embryos, housing the mice, and excellent technical assistance, and members of division of Morphogenesis in NIBB and the Laboratory for Vertebrate Body Plan in RIKEN CDB for valuable discussion. This work was supported by a Grant-in-Aid for Scientific Research, MEXT, Japan to S.A. (18GS0320) and N.U. (22116511, 22127007).

References

Alarcón VB. Cell polarity regulator PARD6B is essential for trophectoderm formation in the preimplantation mouse embryo. Biol Reprod. 2010; 83:347–358. [PubMed: 20505164]

Axelrod JD. Progress and challenges in understanding planar cell polarity signaling. Semin Cell Dev Biol. 2009; 8:964–971. [PubMed: 19665570]

Bassuk AG, Wallace RH, Buhr A, Buller AR, Afawi Z, Shimojo M, Miyata S, Chen S, Gonzalez-Alegre P, Griesbach HL, Wu S, Nashelsky M, Vlader EK, Antic D, Ferguson PJ, Cirak S, Voit T, Scott MP, Axelrod JD, Gurnett C, Daoud AS, Kivity S, Neufeld MY, Mazarib A, Straussberg R, Walid S, Korczym AD, Slusarski DC, Berkovic SF, El-Shanti HI. A homozygous mutation in human PRICKLE1 causes an autosomal-recessive progressive myoclonus epilepsy-ataxia syndrome. Am J Hum Genet. 2008; 83:572–581. [PubMed: 18976727]

Carreira-Barbosa F, Concha ML, Takeuchi M, Ueno N, Wilson SW, Tada M. Prickle1 regulates cell movements during gastrulation and neuronal migration in zebrafish. Development. 2003; 130:4037–4046. [PubMed: 12874125]

Clayton L, Hall A, Johnson MH. A role for Rho-like GTPase in the polarisation of mouse eight-cell blastomeres. Dev Biol. 1999; 205:321–331.

Dard N, Le T, Maro B, Louvet-Vallée S. Inactivation of aPKClambda reveals a context dependent allocation of cell lineages in preimplantation mouse embryos. PLoS One. 2009; 4:e7717. [PubMed: 19890387]

Deans MR, Antic D, Suyama K, Scott MP, Axelrod JD, Goodrich LV. Asymmetric distribution of prickle-like 2 reveals an early underlying polarization of vestibular sensory epithelia in the inner ear. J Neurosci. 2007; 27:3139–3147. [PubMed: 17376975]

Djiane A, Yogev S, Mlodzik M. The apical determinants aPKC and dPatj regulate Frizzled-dependent planar cell polarity in the Drosophila eye. Cell. 2005; 121:621–631. [PubMed: 15907474]

Dollar GL, Weber U, Mlodzik M, Sokol SY. Regulation of Lethal giant larvae by Dishevelled. Nature. 2005; 437:1376–1380. [PubMed: 16251968]

Eckert JJ, Fleming TP. Tight junction biogenesis during early development. Biochim Biophys Acta. 2008; 1778:717–728. [PubMed: 18339299]

Fleming TP, Johnson MH. From egg to epithelium. Annu Rev Cell Biol. 1998; 4:459–485. [PubMed: 3058163]

Goodrich LV. The plane facts of PCP in the CNS. Neuron. 2008; 60:9–16. [PubMed: 18940584]

Goodrich LV, Strutt D. Principles of planar cell polarity in animal development. Development. 2011; 138:1877–1892. [PubMed: 21521735]

Hamatani T, Carter MG, Sharov AA, Ko MS. Dynamics of global gene expression changes during mouse preimplantation development. Dev Cell. 2004; 6:117–131. [PubMed: 14723852]

Houliston E, Pickering SJ, Maro B. Redistribution of microtubules and pericentriolar material during the development of polarity in mouse blastomeres. J Cell Biol. 1987; 104:1299–1308. [PubMed: 3571331]

Jedrusik A, Parfitt DE, Guo G, Skamagki M, Grabarek JB, Johnson MH, Robosin P, Zernicka-Goetz M. Role of Cdx2 and cell polarity in cell allocation and specification of trophectoderm and inner cell mass in the mouse embryo. Genes Dev. 2008; 22:2692–2706. [PubMed: 18832072]

Jedrusik A, Bruce AW, Tan MH, Leong DE, Skamagki M, Yao M, Zernicka-Goetz. Maternally and zygotically provided Cdx2 have novel and critical roles for early development of the mouse embryo. Dev Biol. 2010; 344:66–78. [PubMed: 20430022]

Johnson MH, Chisholm JC, Fleming TP, Houliston E. A role for cytoplasmic determinants in the development of the mouse early embryo? J Embryol Exp Morphol. 1986; 97:97–121. [PubMed: 2442282]

Johnson R, Teh CH, Kunarso G, Wong KY, Srinivasan G, Cooper ML, Volta M, Chan SS, Lipovich L, Pollard SM, Karuturi RK, Wei CL, Buckley NJ, Stanton LW. REST regulates distinct transcriptional networks in embryonic and neural stem cells. PLoS Biol. 2008; 6:e256. [PubMed: 18959480]

Katoh M, Katoh M. Identification and characterization of human PRICKLE1 and PRICKLE2 genes as well as mouse Prickle1 and Prickle2 genes homologous to Drosophila tissue polarity gene prickle. Int J Mol Med. 2003; 11:249–256. [PubMed: 12525887]

Lake BB, Sokol SY. Strabisumus regulates asymmetric cell divisions and cell fate determination in the mouse brain. J Cell Biol. 2009; 185:59–66. [PubMed: 19332887]

Lu CW, Yabuuchi A, Chen L, Viswanathan S, Kim K, Daley GQ. Ras-MAPK signaling promotes trophectoderm formation from embryonic stem cell and mouse embryo. Nat Genet. 2008; 40:921–926. [PubMed: 18536715]

Mapp OM, Walsh GS, Moens CB, Tada M, Prince VE. Zebrafish Prickle1b mediated facial branchiomotor neuron migration via a farnesylation-dependent nuclear activity. Development. 2011; 138:2121–2132. [PubMed: 21521740]

Marikawa Y, Alarcón VB. Establishment of trophectoderm and inner cell mass lineages in the mouse embryo. Mol Reprod Dev. 2009; 76:1019–1032. [PubMed: 19479991]

Maro B, Kubiak J, Gueth C, De Pennart H, Houliston E, Weber M, Antony C, Aghion J. Cytoskeleton organization during oogenesis, fertilization and preimplantation development of the mouse. Int J Dev Biol. 1990; 34:127–137. [PubMed: 2203452]

Maurer-Stroh S, Koranda M, Benetka W, Schneider G, Sirota FL, Eisenhaber F. Towards complete sets of farnesylated and geranylgeranylated proteins. PLoS Comput Biol. 2007; 3:e66. [PubMed: 17411337]

Montcouquiol M, Rachel RA, Lanford PJ, Copeland NG, Jenkins NA, Kelley MW. Identification of Vangl2 and Scrb1 as planar polarity genes in mammals. Nature. 2003; 423:173–177. [PubMed: 12724779]

Montcouquiol M, Sana M, Huss D, Kach J, Dickman JD, Forge A, Rachel RA, Copeland NG, Jenkins NA, Bogani D, Murdoch J, Warchol ME, Wenthold RJ, Kelley MW. Asymmetric localization of Vangl2 and Fzd3 indicated novel mechanisms for planar cell polarity in mammals. J Neurosci. 2006; 26:5265–5275. [PubMed: 16687519]

Nagy, A.; Gertsenstein, M.; Vintersten, K.; Behringer, RR. Manipulating the mouse embryo a laboratory manual. 3. Cold Spring Harbor Laboratory Press; Cold Spring Harbor, NY: 2003.

Nelson WJ. Remodeling epithelial cell organization: transitions between font-rear and apical-basal polarity. Cold Spring Harb Perspect Biol. 2009; 1:a000513. [PubMed: 20066074]

Nishioka N, Yamamoto S, Kiyonari H, Sato H, Sawada A, Ota M, Nakao K, Sasaki H. Tead4 is required for specification of trophectoderm in pre-implantation mouse embryos. Mech Dev. 2008; 125:270–283. [PubMed: 18083014]

Nishioka N, Inoue K, Adachi K, Kiyonari H, Ota M, Ralston A, Yabuta N, Hirahara S, Stephenson RO, Ogonuki N, Kurihara H, Morin-Kensicki EM, Nojima H, Rossant J, Nakao K, Niwa H, Sasaki H. The Hippo signaling pathway components Lats and Yap pattern Tead4 activity to distinguish mouse trophectoderm from inner cell mass. Dev Cell. 2009; 16:398–410. [PubMed: 19289085]

Nishita M, Enomoto M, Yamagata K, Minami Y. Cell/tissue-tropic function of Wnt5a signaling in normal and cancer cells. Trends Cell Biol. 2010; 6:346–354. [PubMed: 20359892]

Plusa B, Frankenberg S, Chalmers A, Hadjantonakis AK, Moore CA, Papalopulu N, Papaioannou VE, Glover DM, Zernicka-Goetz M. Downregulation of Par3 and aPKC function directs cells towards the ICM in the preimplantation mouse embryo. J Cell Sci. 2005; 118:505–515. [PubMed: 15657073]

Ralston A, Rossant J. Cdx2 acts downstream of cell polarization to cell-autonomously promote trophectoderm fate in the early mouse embryo. Dev Biol. 2008; 313:614–629. [PubMed: 18067887]

Rossant J, Tam PP. Blastocyst lineage formation, early asymmetries and axis patterning in the mouse. Development. 2009; 136:701–713. [PubMed: 19201946]

Sasaki H. Mechanisms of trophectoderm fate specification in preimplantation mouse development. Dev Growth Differ. 2010; 52:263–273. [PubMed: 20100249]

Sepich DS, Usmani M, Pawlicki S, Solnica-Krezel L. Wnt/PCP signaling controls intracellular position of MTOCs during gastrulation convergence and extension movements. Development. 2011; 138:543–552. [PubMed: 21205798]

Shimojo M, Hersh LB. REST/NRSF-interacting LIM domain protein, a putative nuclear translocation receptor. Mol Cell Biol. 2003; 23:9025–9031. [PubMed: 14645515]

Shimojo M, Hersh LB. Characterization of the REST/NRSF-interacting LIM domain protein (RILP): localization and interaction with REST/NRSF. J Neurochem. 2006; 96:1130–1138. [PubMed: 16417580]

Simons M, Mlodzik M. Planar cell polarity signaling: from fly development to human disease. Annu Rev Genet. 2008; 42:517–540. [PubMed: 18710302]

Strumpf D, Mao CA, Yamanaka Y, Ralston A, Chawengsaksophak K, Beck F, Rossant J. Cdx2 is required for correct cell fate specification and differentiation of trophectoderm in the mouse blastocyst. Development. 2005; 132:2093–2102. [PubMed: 15788452]

Surani MA, Kimber SJ, Osborn JC. Mevalonate reverses the developmental arrest of preimplantation mouse embryos by compactin, an inhibitor of HMG Co A reductase. J Embryol Exp Morph. 1983; 75:205–223. [PubMed: 6886611]

Suzuki A, Ohno S. The PAR-aPKC system: lessons in polarity. J Cell Sci. 2006; 119:979–987. [PubMed: 16525119]

Takeuchi M, Nakabayashi J, Sakaguchi T, Yamamoto TS, Takahashi H, Takeda H, Ueno N. The prickle-related gene in vertebrates is essential for gastrulation cell movements. Curr Biol. 2003; 13:674–679. [PubMed: 12699625]

Tao H, Suzuki M, Kiyonari H, Abe T, Sasaoka T, Ueno N. Mouse prickle1, the homolog of a PCP gene, is essential for epiblast apical-basal polarity. Proc Natl Acad Sci U S A. 2009; 106:14426–14431. [PubMed: 19706528]

Tao H, Manak R, Sowers L, Mei X, Kiyonari H, Abe T, Dahdaleh NS, Yang T, Wu S, Chen S, Fox MH, Gurnett C, Montine T, Bird T, Shaffer LG, Rosenfeld JA, McConnell J, Madan-Khetarpal S, Berry-Kravis E, Griesbach H, Saneto R, Scott MP, Antic D, Reed J, Boland R, Ehaideb SN, El-Shanti H, Mahajan VB, Ferguson PJ, Axelrod JD, Lehesjoki AE, Fritzsch B, Slusarski DC, Wemmie J, Ueno N, Bassuk AG. Mutations in prickle orthologs cause seizures in flies, mice, and humans. Am J Hum Genet. 2011; 88:138–149. [PubMed: 21276947]

Varelas X, Samavarchi-Tehrani P, Narimatsu M, Weiss A, Cockburn K, Larsen BG, Rossant J, Warana JL. The Crumbs complex couples cell density sensing to Hippo-dependent control of the TGF-β-SMAD pathway. Dev Cell. 2010; 19:831–844. [PubMed: 21145499]

Veeman MT, Slusarski DC, Kaykas A, Louie SH, Moon RT. Zebrafish prickle, a modulator of noncanonical Wnt/Fz signaling, regulates gastrulation movements. Curr Biol. 2003; 13:680–685. [PubMed: 12699626]

Vinot S, Le T, Ohno S, Pawson T, Maro B, Louvet-Vallée S. Asymmetric distribution of PAR proteins in the mouse embryo begins at the 8-cell stage during compaction. Dev Biol. 2005; 282:307–319. [PubMed: 15950600]

Wansleeben C, Meijlink F. The planar cell polarity in vertebrate development. Dev Dyn. 2011; 240:616–626. [PubMed: 21305650]

Xie H, Tranguch S, Jia X, Zhang H, Das SK, Dey SK, Kuo CJ, Wang H. Inactivation of nuclear Wnt-beta-catenin signaling limits blastocyst competency for implantation. Development. 2008; 135:717–727. [PubMed: 18199579]

Yagi R, Kohn MJ, Karavanova KJ, Kaneko KJ, Vullhorst D, DePamphilis ML, Buonanno A. Transcription factor TEAD4 specifies the trophectoderm lineage at the beginning of mammalian development. Development. 2007; 134:3827–3836. [PubMed: 17913785]

Yamagata K, Yamazaki T, Yamashita M, Hara Y, Ogonuki N, Ogura A. Noninvasive visualization of molecular events in the mammalian zygote. Genesis. 2005; 43:71–79. [PubMed: 16100711]

Yamanaka Y, Ralston A, Stephenson RO, Rossant J. Cell and molecular regulation of the mouse blastocyst. Dev Dyn. 2006; 235:2301–2314. [PubMed: 16773657]

Zallen JA. Planar polarity and tissue morphogenesis. Cell. 2007; 129:1051–1063. [PubMed: 17574020]

Zernicka-Goetz M, Morris SA, Bruce AW. Making a firm decision: multifaceted regulation of cell fate in the early mouse embryo. Nat Rev Genet. 2009; 10:467–477. [PubMed: 19536196]

Highlights

- Pk2 protein was mainly localized in the nucleus from 2-cell stage up to the 8-cell stage
- *Pk2*$^{-/-}$ embryos failed to form a blastocyst cavity.
- *Pk2* mediates microtubule redistribution within the cell cortex during compaction
- The loss of *Pk2* disrupts expression and localization of AB polarity components
- The nuclear retention of Pk2 is required for the establishment of cell polarity

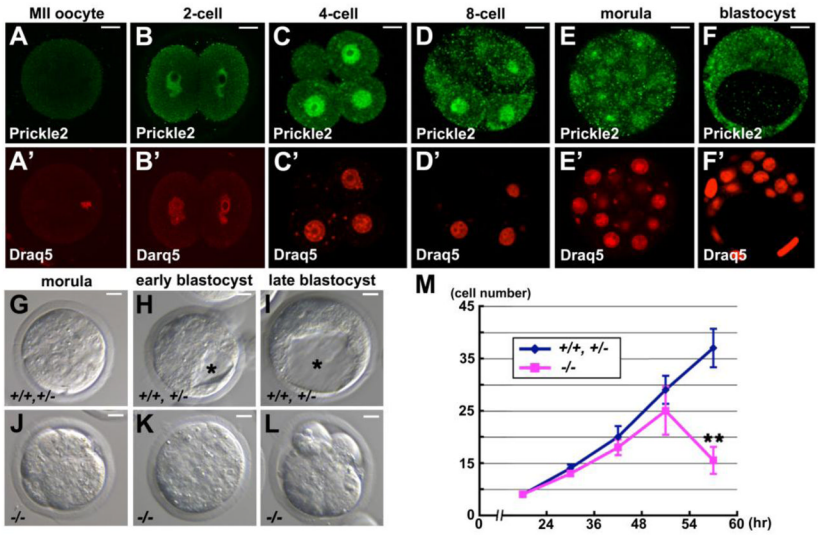

Fig. 1.

Expression of Pk2 and the gross phenotypes of *Pk2*$^{-/-}$ embryos. (A-F) Expression of Pk2 protein at serial stages. (A'-F') Nuclei were stained with Draq5. Images were taken of a central plane through the embryo. (G-L) DIC images of control (*Pk2*$^{+/+}$ and/or *Pk2*$^{+/-}$ embryos) and *Pk2*$^{-/-}$ embryos at serial stages. (M) The number of nuclei in control and *Pk2*$^{-/-}$ embryos were counted by staining the nuclei with Draq5. The number of embryos analyzed at each stage were, respectively: for control, n = 5, 6, 7, 6, 8; and *Pk2*$^{-/-}$, n = 4, 4, 5, 6, 6. Asterisk indicates the blastocyst cavity. Data are represented as means and the error bars represent the a.d.. Scale bars, 10 μm.

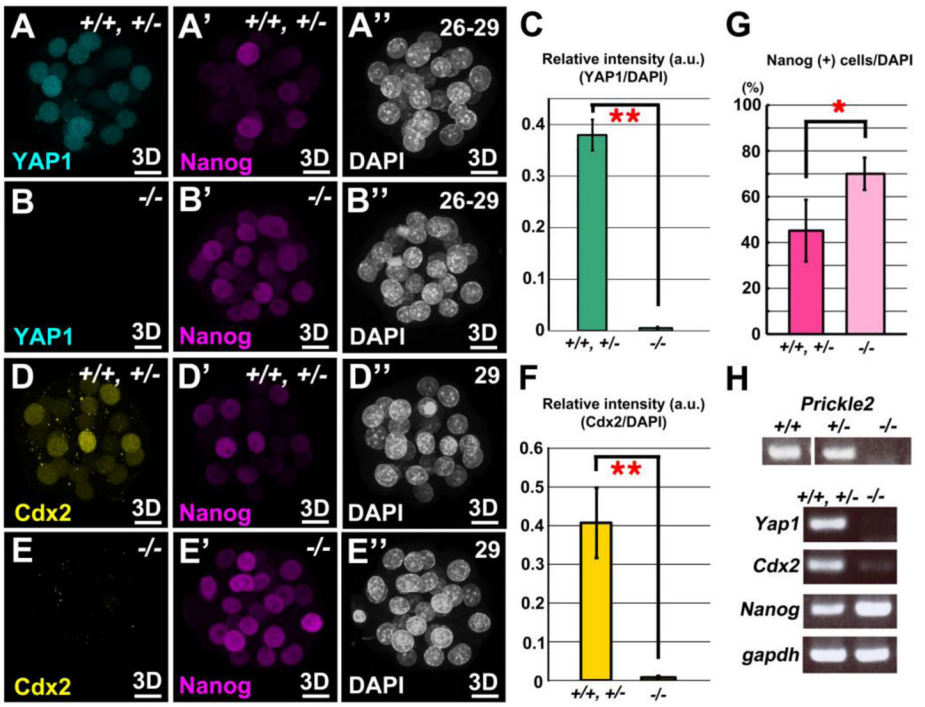

Fig. 2.

Failure of TE lineage specification in *Pk2*$^{-/-}$ embryos. (A-B") Double IHC for YAP1 and Nanog at the stages indicated. (C) Quantification of relative intensity of YAP1 to DAPI staining in control and *Pk2*$^{-/-}$ embryos, respectively. For each embryo, nuclei of five outer cells were arbitrarily chosen for fluorescence intensity measurement, and the mean s.d. from all the measurements for each genotype are presented in the graph. (D-E") Double IHC for Cdx2 and Nanog at the stages indicated. (F) Quantification of relative intensity of Cdx2 to DAPI staining in control and *Pk2*$^{-/-}$ embryos, respectively. For each embryo, nuclei of five outer cells were arbitrarily chosen for fluorescence intensity measurement, and the mean s.d. from all the measurements for each genotype are presented in the graph. (G) Measurement of Nang-positive cells in *Pk2*$^{-/-}$ embryos. Nanog fluorescence levels were normalized by DAPI staining levels for each nucleus. (H) Absence of TE marker expression in *Pk2*$^{-/-}$ embryos. RT-PCR was performed using *RNAs* isolated from each genotyped embryo at the late-morula stage. (A"-E") The number of blastomeres was counted by DAPI staining. Each image was a Z-series projection of the confocal sections of embryos (3D). Error bars indicate s.d. (n>8). ***P*<0.01 and **P*<0.05 by Student's *t*-test. Scale bars, 10 μm.

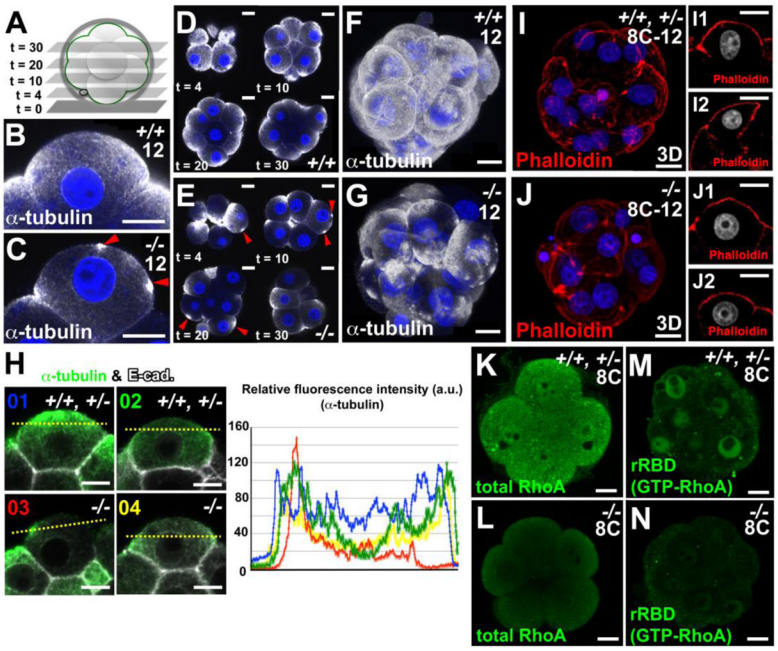

Fig. 3.

Pk2 mediates redistribution of the microtubular architecture within the cell cortex during compaction. (A) Z-value indicates the optical section number from the bottom, as shown in the planes in D and E. (B-G) IHC for α-tubulin in the control and $Pk2^{-/-}$ embryos. Red arrowheads indicate the irregular apical accumulation of α-tubulin staining (C and E). Each image was taken in a z-projected plane (t = 10) (B and C), in each z-projected planes (t = 4, 10, 20, 30), respectively (D and E). Each image was a Z-series projection of the confocal sections of embryos, respectively (F and G). (H) Double IHC for α-tubulin and E-cadherin. Fluorescence intensity of the α-tubulin signal scanned across cell-cell boundaries between control (type 1 or type 2, 80% or 20%, 66/83 or 17/83 blastomeres, n = 16 embryos) and $Pk2^{-/-}$ (type 3, 60%, 28/47 blastomeres, type 4, 40%, 19/47 blastomeres, n = 8 embryos) blastomeres (yellow dot line). (I-J2) Rhodamine phalloidin staining. Nuclei (blue or gray) were stained with DAPI. Each image was a Z-series projection of the confocal sections of embryos (I and J) or was taken in a central plane through the embryo (I1, I2, J1 and J2). (K-N) IHC for total and GTP-bound (active) RhoA. Scale bars, 10 μm.

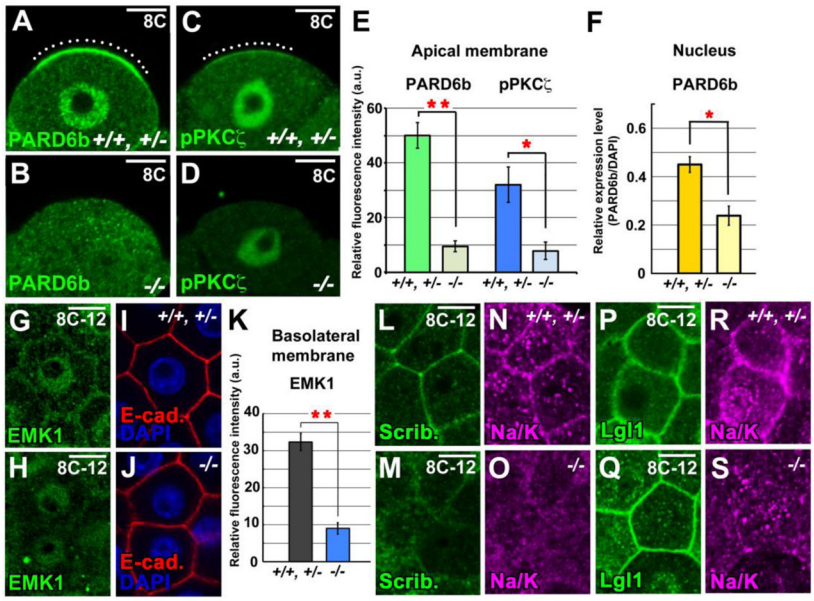

Fig. 4.

Pk2 regulates the AB polarity during compaction. (A and B) IHC for PARD6b, (C and D) IHC for phosphorylated PKCζ (pPKCζ). White dotted lines show the distinct PARD6b or pPKCζ signals on apical membrane of the control embryos. (E) Fluorescence intensity of the PARD6b or pPKCζ signal scanned across the apical cell cortex and (F) of the nuclear PARD6b at 8-cell stage, respectively. (G-J) Double IHC for EMK1 and E-cadherin. Nuclei (blue) were stained with DAPI. (K) Fluorescence intensity of the EMK1 signal of scanned cell-cell boundaries marked by E-cadherin staining. These signals were normalized to the fluorescence intensity of E-cadherin. (L-O) Double IHC for Scribble and Na^+/K^+ ATPase α1 subunit. (P-S) Double IHC for Lgl1 and Na^+/K^+ ATPase α1 subunit. Each image was taken a middle plane of the confocal sections of embryos. Error bars indicate s.d. (n>8). $^{**}P<0.01$ and $^{*}P<0.05$ by Student's *t*-test. Scale bars, 10 μm.

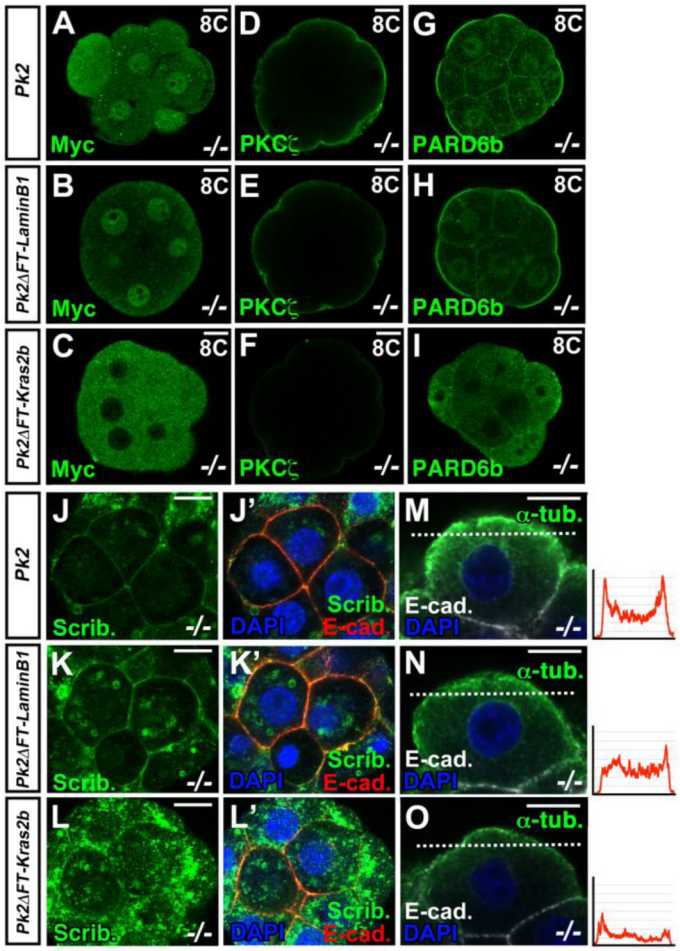

Fig. 5.

Nuclear translocation of Pk2 is prerequisite for the establishment of cell polarity. (A-I) IHC for Myc, PKCζ and PARD6b in embryos receiving injections of Myc-tagged *Pk2 RNA*, or Myc-tagged *RNA* for *Pk2* in which the C-terminus was replaced with that of *Lamin B1* or *Kras2*, at the indicated stages in $Pk2^{-/-}$ embryos. (J-L') Double IHC for Scrib and E-cadherin in $Pk2^{-/-}$ embryos receiving injections of various mutant *Pk2 RNAs* at the compacted 8-cell stage. (M-O) Double IHC for α-tubulin and E-cadherin in $Pk2^{-/-}$ embryos receiving injections of various mutant *Pk2 RNAs* at the compacted 8-cell stage. Each graph indicates immunofluorescence intensity of the α-tubulin signal scanned by a white dot line for each injected blastomeres. Scale bars, 10 μm.